Hindawi
Mathematical Problems in Engineering
Volume 2020, Article ID 6638425, 10 pages
https://doi.org/10.1155/2020/6638425

Research Article

STAP Based on Toeplitz Covariance Matrix Reconstruction for Airborne Radar

Mingxin Liu, Lin Zou, Xuelian Yu, Yun Zhou, and Xuegang Wang

School of Information and Communication Engineering, University of Electronic Science and Technology of China, Chengdu 611731, China

Correspondence should be addressed to Lin Zou; zoulin_ee706@uestc.edu.cn

Received 6 October 2020; Revised 7 December 2020; Accepted 12 December 2020; Published 23 December 2020

Academic Editor: David Bigaud

We consider the problem of clutter covariance matrix (CCM) estimation for space-time adaptive processing (STAP) radar in the small sample. In this paper, a fast efficient algorithm for CCM reconstruction is proposed to overcome this shortcoming for the linear structure. Particularly, we present a low-rank matrix recovery (LRMR) question about CCM estimation based on the Toeplitz structure of CCM and the prior knowledge of the noise. The closed-form solution is obtained by relaxing the nonconvex LRMR problem that the trace norm replaces the rank norm. The target can then be efficiently detected by using the recovered CCM according to the STAP theorem. We also analyze the algorithm model under the linear structure in the presence of unknown mutual coupling. It is shown that our method can obtain accurate CCM in the small sample, with even higher accuracy than the traditional algorithms in the same number of samples. It also can reduce the coupling effect and obtain more degrees of freedom (DOF) with limited sensors and pulses by utilizing sparse linear structure (SLS) and improve angle and Doppler resolutions. Finally, numerical simulations have verified the effectiveness of the proposed method in comparison with some of the existing methods.

1. Introduction

Space-time adaptive processing (STAP) which has an excellent performance on clutter suppression and targets detection plays a fundamental role in radar [1–3]. In the practical application of STAP, the system can calculate the ideal weight vector and then obtain the optimal filter output responses based on the clutter covariance matrix (CCM) estimated with its adjacent distance cell snapshots. Therefore, the training snapshots play an important role in the adaptive radar system. In practice, the system needs a large number of uniform training snapshots to obtain the reliable and accurate CCM. It is difficult for radar to meet the above-mentioned condition in a heterogeneous environment, especially in a small sample [4].

The problem of sample size for STAP radar has received considerable attention recently. These works can be classified into two categories. The first category is the failure to take advantage of the prior knowledge to reduce sample size, which can be defined as the generalized reduced sample size method. For the dimension reduction [5–7] and reduced rank STAP [8], the sample size is twice the reduced dimension or clutter rank, but it is still large. The direct data domain method only uses test unit data to suppress clutter at the cost of freedom loss, which is only suitable for uniform linear array and planar array [9]. Sparse recovery STAP obtains the high CCM accuracy by solving underdetermined equation [10]. It can suppress clutter very well with a small number of samples, but the existing sparse recovery STAP has some problems such as sparsity, dispersion, and base mismatch, which will affect the accuracy of the CCM.

The second category approaches sample size by fully utilizing various prior knowledge. In [11], the unknown covariance matrix contained the noise was achieved by the knowledge-aided Bayesian framework and a set of training samples. A knowledge-aided model that cared for the nonhomogeneous characteristics of the disturbance with distributed MIMO radar considered in [12] solves the problems of nonhomogeneous environments and insufficient training samples. In addition to the above methods

applying the prior statistical distribution, there are also algorithms employing the prior environmental data [13, 14]. However, if the prior knowledge is inaccurate, the system will create inaccurate estimates for the CCM in target detecting, leading to poor performance. To avoid this, we reduce sampling size by means of the structure of CCM, including power spectral density [13, 15], symmetry [16], and eigenstructure [17]. Notably, the CCM of stationary random signals is Hermitian and Toeplitz; the various estimation and approximation techniques of the Toeplitz matrix have been studied in the last ten years. However, many Toeplitz matrix estimation techniques are based on the assumption of large sample sizes [18].

In this paper, we investigate the STAP radar CCM reconstruction (TCMR-STAP) in uniform linear structure (ULS) and sparse linear structure (SLS), by taking into account the small sample constraint as well as mutual coupling effect. More specifically, the CCM restoration of ULS and SLS is proposed based on the Toeplitz structure. In particular, we first propose a low-rank matrix recovery (LRMR) problem based on Toeplitz structure CCM reconstruction which is then relaxed by replacing the rank norm with the trace norm and calculate the reconstructed CCM by a fast and feasible method. Afterwards, the CCM is used to detect the target effectively according to the STAP theory. Moreover, we reduce the influence of mutual coupling by utilizing the SLS and increase system of degrees of freedom (DOF) under the limited sensors and pulses by difference operation. Simulations demonstrate the theoretical derivations and advantages of the proposed TCMR-STAP algorithm.

The remainder of this paper is organized as follows: in Section 2, we introduce the signal model with the ULS and SLS system. Section 3 gives the signal model under the mutual coupling and a fast closed CCM reconstruction method. In Section 4, simulation results and discussions prove its superiority. Finally, Section 5 gains the conclusions.

Notations: $(\cdot)^T$, $(\cdot)^H$ are transpose and complex conjugate transpose operators, respectively. $\otimes$, $E(\cdot)$, and $|\cdot|$ stand for the Kronecker product, the expected value, and the absolute value, respectively. $\mathbf{I}_M$ is the $M \times M$ identity matrix, and $\mathrm{diag}(\mathbf{a})$ represents a diagonal matrix whose diagonal elements are the column vector $\mathbf{a}$. $\mathrm{Toeplitz}(\mathbf{t})$ is the symmetric Toeplitz matrix consisting of the vector $\mathbf{t}$. $\mathrm{vec}(\cdot)$ represents the vectorization operator. $\mathrm{tr}[\cdot]$ and $\mathrm{rank}[\cdot]$ stand for the matrix trace and rank, respectively. $\|\cdot\|_2$ denotes the l_2 norm. $(\cdot)^*$ denotes the adjoint operator. $\mathscr{R}(\cdot)$ and $\mathscr{I}(\cdot)$ are the real and imaginary operators, respectively. †denotes the pseudoinversion operator.

2. Signal Model

2.1. The ULS System. Consider a phased array radar system that employs an N sensors uniform linear array (ULA) with intersensors spacing d and M transmitting pulses with fixed pulse repetition interval (PRI) T_r during a coherent processing interval (CPI), which is called the ULS system. The velocity of the radar platform is v, and the radar wavelength is λ. The clutter at each range bin can be modeled as the superposition of N_c independent clutter patches. The ith clutter patch spatial and temporal steering vectors are, respectively, given as

$$\begin{aligned} v\left(\varphi_{c,i}\right) &= \left[1, e^{2\pi j\varphi_{c,i}}, \ldots, e^{2\pi j(N-1)\varphi_{c,i}}\right]^T, \\ v\left(f_{c,i}\right) &= \left[1, e^{2\pi j f_{c,i}}, \ldots, e^{2\pi j(M-1) f_{c,i}}\right]^T, \end{aligned} \tag{1}$$

where $\varphi_{c,i}$ and $f_{c,i}$ are the normalized angle and Doppler frequency of the ith clutter patch, respectively. Therefore, the corresponding space-time steering vector can be calculated by

$$\mathbf{v}\left(\varphi_{c,i}, f_{c,i}\right) = \mathbf{v}\left(\varphi_{c,i}\right) \otimes \mathbf{v}\left(f_{c,i}\right). \tag{2}$$

The space-time clutter plus noise snapshot from a range bin without the ranger ambiguity is denoted as

$$\mathbf{x}_u = \sum_{i=1}^{N_c} a_{c,i}\mathbf{v}\left(\varphi_{c,i}, f_{c,i}\right) + \mathbf{n}, \tag{3}$$

where $a_{c,i}$ represents the ith clutter patch complex amplitude and $\mathbf{n}$ is the Gaussian white noise vector whose power is σ_n^2. Thus, the clutter plus noise covariance matrix (CNCM) based on (3) can be calculated by

$$\mathbf{R}_u = E\left[\mathbf{x}_u\mathbf{x}_u^H\right] = \mathbf{V}\mathbf{P}\mathbf{V}^H + \sigma_n^2\mathbf{I}_{NM} = \mathbf{R}_c + \sigma_n^2\mathbf{I}_{NM}, \tag{4}$$

where $\mathbf{V} = [\mathbf{v}(\varphi_{c,1}, f_{c,1}), \mathbf{v}(\varphi_{c,2}, f_{c,2}), \ldots, \mathbf{v}(\varphi_{c,N_c}, f_{c,N_c})]$ denotes the clutter space-time steering matrix, and the clutter power matrix is $\mathbf{P} = \mathrm{diag}[p_1, p_2, \ldots, p_{N_c}]^T$, $p_i = E(|a_{c,i}|^2)$. The CCM $\mathbf{R}_c = \mathbf{V}\mathbf{P}\mathbf{V}^H$ is a block Toeplitz matrix determined by the vectors $\mathbf{u} = [\mathbf{u}^{(1)T}; \ldots; \mathbf{u}^{(M)T}]^T$ and $\mathbf{v} = [\mathbf{v}^{(1)T}; \ldots; \mathbf{v}^{(M)T}]^T$, where $\mathbf{u}^{(n)} = [u_1^{(n)}; \ldots; u_N^{(n)}]^T$ and $\mathbf{v}^{(n)} = [v_1^{(n)}; \ldots; v_{N-1}^{(n)}]^T$ [2]. Thus, the CCM $\mathbf{R}_c$ becomes block Toeplitz:

$$\mathbf{R}_c(\mathbf{u}, \mathbf{v}) = \begin{bmatrix} \mathbf{R}^{(1)} & \mathbf{R}^{(2)} & \cdots & \mathbf{R}^{(M)} \\ \mathbf{R}^{(-2)} & \mathbf{R}^{(1)} & \cdots & \mathbf{R}^{(M-1)} \\ \vdots & \vdots & \ddots & \vdots \\ \mathbf{R}^{(-M)} & \mathbf{R}^{(-(M-1))} & \cdots & \mathbf{R}^{(1)} \end{bmatrix}, \tag{5}$$

where the spatial covariance matrix $\mathbf{R}^{(n)} \in C_{N\times N}$ is a Toeplitz matrix determined by $\mathbf{u}^{(n)}$ and $\mathbf{v}^{(n)}$, given by

$$\mathbf{R}^{(n)} = \begin{bmatrix} u_1^{(n)} & v_1^{(n)} & \cdots & v_{N-1}^{(n)} \\ u_2^{(n)} & u_1^{(n)} & \cdots & v_{N-2}^{(n)} \\ \vdots & \vdots & \ddots & \vdots \\ u_N^{(n)} & u_{N-1}^{(n)} & \cdots & u_1^{(n)} \end{bmatrix}. \tag{6}$$

2.2. The SLS System. For the SLS system, we assume that the numbers of sensors and pulses are set to N_s and M_s, respectively, and other parameters are the same as those of the ULS system. The sensor locations of the sparse linear array (SLA) are given by

$$\mathrm{A} = \left\{0, A_1, \ldots, A_{N_s-1}\right\} \subset \{0, \ldots, N-1\}, \tag{7}$$

and the sparse linear pulse (SLP) locations are

$$\mathbb{P} = \left\{0, P_1, \ldots, P_{M_s-1}\right\} \subset \{0, \ldots, M-1\}. \tag{8}$$

Thus, the spatial and temporal steering vectors of the ith clutter patch are

$$\begin{aligned} \mathbf{v}_s\left(\varphi_{c,i}\right) &= \left[1, e^{2\pi j A_1 \varphi_{c,i}}, \ldots, e^{2\pi j A_{N_S-1}\varphi_{c,i}}\right]^T, \\ \mathbf{v}_s\left(f_{c,i}\right) &= \left[1, e^{2\pi j P_1 f_{c,i}}, \ldots, e^{2\pi j P_{M_S-1} f_{c,i}}\right]^T, \end{aligned} \tag{9}$$

respectively. Meanwhile, the space-time steering vector of the ith clutter patch can be computed by

$$\mathbf{v}_s\left(\varphi_{c,i}, f_{c,i}\right) = \mathbf{v}_s\left(\varphi_{c,i}\right) \otimes \mathbf{v}_s\left(f_{c,i}\right). \tag{10}$$

Furthermore, the space-time clutter plus noise snapshot from a range bin without the ranger ambiguity can be written as

$$\mathbf{x}_{us} = \sum_{i=1}^{N_c} a_{c,i} \mathbf{v}_s\left(\varphi_{c,i}, f_{c,i}\right) + \mathbf{n}. \tag{11}$$

Definition 1 (difference coarray). For an array specified by an integer set $\mathbf{A}$, its difference coarray D_A is defined as

$$\mathrm{D}_A = \left\{A_i - A_j | A_i, A_j \in \mathrm{A}, A_i \geq A_j\right\}. \tag{12}$$

New set D_{AO} consists of different elements of D_A. The array is a redundant array if $\mathrm{D}_{AO} = \{0, 1, \ldots, N-1\}$. Generally, the array can be classified into the ULA and SLA from the geometry. It is easy to see that the ULA itself is a redundant array, and the SLA is a redundant array only if the prerequisite mentioned previously is met.

Definition 2 (difference copulse). Similarly, a pulse location is an integer set $\mathbb{P}$ and its difference copulse D_P is

$$\mathrm{D}_P = \left\{P_i - P_j | P_i, P_j \in \mathbb{P}, P_i \geq P_j\right\}. \tag{13}$$

When $\mathrm{D}_{PO} = \{0, 1, \ldots, M-1\}$ which is made up of the different elements of D_P, the pulse is defined as a redundant pulse. Here, we can divide the pulse into the uniform linear pulse (ULP) and SLP. Normally the ULP is always a redundant pulse, but the SLP needs to meet $\mathrm{D}_{PO} = \{0, 1, \ldots, M-1\}$. This paper only considers the redundancy structure.

According to the above theory, further analysis indicates that $\mathbf{v}_s(\varphi_{c,i})$ and $\mathbf{v}_s(f_{c,i})$ can be written as

$$\begin{aligned} \mathbf{v}_s\left(\varphi_{c,i}\right) &= \Gamma_A \mathbf{v}\left(\varphi_{c,i}\right), \\ \mathbf{v}_s\left(f_{c,i}\right) &= \Gamma_P \mathbf{v}\left(f_{c,i}\right), \end{aligned} \tag{14}$$

respectively, where the nth rows of the array selection matrix $\Gamma_A \in \{0,1\}^{N_S \times N}$ are all zeros except for a single 1 in the A_nth position, and $\Gamma_P \in \{0,1\}^{M_P \times M}$ means the pulse selection matrix where the element of the mth row is 1 at the P_mth position and the remaining elements are all 0.

Thus, the CNCM of the SLS can be estimated by

$$\begin{aligned} \mathbf{R}_{us} &= E\left[\mathbf{x}_{us}\mathbf{x}_{us}^H\right] = \sum_{i=1}^{N_c} E\left(\left|a_{c,i}\right|^2\right) \mathbf{v}_s\left(\varphi_{c,i}, f_{c,i}\right) \mathbf{v}_s^H\left(\varphi_{c,i}, f_{c,i}\right) \\ &\quad + \sigma_n^2 \mathbf{I}_{N_s M_s} \\ &= \Gamma \mathbf{R}_c \Gamma^H + \sigma_n^2 \Gamma\Gamma^H = \mathbf{R}_{cs} + \sigma_n^2 \Gamma\Gamma^H, \end{aligned} \tag{15}$$

where $\Gamma = \Gamma_A \otimes \Gamma_P$ and $\mathbf{R}_{cs} = \Gamma \mathbf{R}_c \Gamma^H$. The previous equation degenerates into the CNCM of the ULS if $\Gamma = \mathbf{I}$. In other words, the ULS is one of the special forms of the SLS.

3. The Proposed Method

In this section, we describe in detail the design of the proposed TCMR-STAP algorithm with Toeplitz covariance matrix reconstruction. Whether the ULS or SLS, we can reconstruct the CCM quickly and precisely. In order to fully reflect the value of the TCMR-STAP algorithm, we consider the influence of the mutual coupling among sensors.

3.1. Mutual Coupling. In the practical radar system, the received signal has changed owing to the electromagnetic coupling among the sensors. According to the electromagnetic coupling principle, the larger the intersensors spacing is, the smaller the coupling effect is. If the intersensors spacing is greater than a few wavelengths, the effect of coupling can be ignored. Therefore, we can describe the mutual coupling effect utilizing the weight function $w(n)$ of an array. $w(n)$ of an array $\mathbf{A}$ is defined as the number of element pairs generating the coarray index n, namely, [19]

$$w(n) = \left|\left\{\left(A_i, A_j\right) \in \mathrm{A}^2, A_i - A_j = n\right\}\right|, \quad n \in \mathrm{D}_{AO}. \tag{16}$$

The first three weight functions of the ULA from (16) are $w(1) = N-1$, $w(2) = N-2$, and $w(3) = N-3$, $N \geq 3$. It is clear that the SLA have much smaller weight functions compared to the ULA. This means that the mutual coupling effect of SLA is relatively small.

Supposing that the mutual coupling coefficient is zero when the distance between two sensors is larger than Bd [20], B is a positive integer. Then, the mutual coupling matrix (MCM) of the ULA is formulated as

$$\mathbf{C} = \mathrm{Toeplitz}\left\{\left[\mathbf{c}^T, 0_{1\times(N-B)}\right]\right\}, \tag{17}$$

where $\mathbf{c} = [c_0, c_1, c_2, \ldots, c_B]^T$ satisfy $|c_B| < \cdots < |c_1| < |c_0| = 1$ and $0_{1\times(N-B)}$is a $1 \times (N-B)$ zero vector.

There are also more sophisticated mutual coupling models [21]. In theory, all of the above models can be applied to the SLA to be discussed in this paper and attain excellent performance. As a matter of fact, the MCM is unknown. If the coupling effect is ignored completely in the design of the

STAP filter, the performance of radar detection will degrade or even be disabled.

3.2. The ULS System with Mutual Coupling. The mutual coupling effect in the STAP radar will distort the space-time steering vector. We need to give careful consideration to the mutual coupling effect in actual radar systems. For the ULS system, the clutter plus noise data $\mathbf{x}_{um}$ in the presence of mutual coupling can be modified as [20]

$$\mathbf{x}_{um} = \sum_{i=1}^{N_c} a_{c,i}\mathbf{v}_m\left(\varphi_{c,i}, f_{c,i}\right) + \mathbf{n}, \tag{18}$$

where $\mathbf{v}_m(\varphi_{c,i}, f_{c,i}) = \mathbf{v}_m(\varphi_{c,i}) \otimes \mathbf{v}(f_{c,i})$ is the ith clutter patch space-time steering vector under the mutual coupling in which $\mathbf{v}_m(\varphi_{c,i}) = \mathbf{C}\mathbf{v}(\varphi_{c,i})$ indicates the corresponding spatial steering vector. Therefore, by introducing the MCM $\mathbf{C}$, (4) can be modified as

$$\mathbf{R}_{um} = E\left[\mathbf{x}_{um}\mathbf{x}_{um}^H\right] = \mathbf{V}_m\mathbf{P}\mathbf{V}_m^H + \sigma_n^2\mathbf{I}_{NM} = \mathbf{R}_{cm} + \sigma_n^2\mathbf{I}_{NM}, \tag{19}$$

where $\mathbf{V}_m = [\mathbf{v}_m(\varphi_{c,1}, f_{c,1}), \mathbf{v}_m(\varphi_{c,2}, f_{c,2}), \ldots, \mathbf{v}_m(\varphi_{c,N_c}, f_{c,N_c})]$ is the clutter space-time steering matrix considering the mutual coupling among the physical sensors; the corresponding CCM denotes $\mathbf{R}_{cm} = \mathbf{V}_m\mathbf{P}\mathbf{V}_m^H$. Here, by comparing (4) with (19), we find

$$\mathbf{R}_{cm} = \mathbf{Z}\mathbf{R}_c\mathbf{Z}^H, \tag{20}$$

where $\mathbf{Z} = \mathbf{C} \otimes \mathbf{I}_M$.

3.3. The SLS System with Mutual Coupling. In this section, we extend the coupling effect to the SLS, which can be regarded as a subset of ULS. The magnitudes of coupling coefficients are inversely proportional to intersensors spacing. As a result, the SLS has been less affected by the mutual coupling due to its relatively sparse array. By considering the mutual coupling, (11) can be changed as

$$\mathbf{x}_{usm} = \sum_{i=1}^{N_c} a_{c,i}\mathbf{v}_{sm}\left(\varphi_{c,i}, f_{c,i}\right) + \mathbf{n} = \sum_{i=1}^{N_c} a_{c,i}\left[\mathbf{C}\Gamma_A\mathbf{v}\left(\varphi_{c,i}\right)\right] \otimes \left[\Gamma_P\mathbf{v}\left(f_{c,i}\right)\right] + \mathbf{n}, \tag{21}$$

where $\mathbf{v}_{sm}(\varphi_{c,i}, f_{c,i}) = \mathbf{v}_{sm}(\varphi_{c,i}) \otimes \mathbf{v}_s(f_{c,i})$ is the space-time steering vector of the ith clutter patch with mutual coupling. $\mathbf{v}_{sm}(\varphi_{c,i}) = \mathbf{C}\mathbf{v}_s(\varphi_{c,i})$ denotes the corresponding of the spatial steering vector. Furthermore, the CNCM of the SLS with mutual coupling has the form as follows:

$$\mathbf{R}_{usm} = E\left[\mathbf{x}_{usm}\mathbf{x}_{usm}^H\right] = \mathbf{R}_{c\Omega} + \sigma_n^2\mathbf{I}_{N_sM_s} = \mathbf{R}_{c\Omega} + \mathbf{I}_\Gamma, \tag{22}$$

where

$$\begin{aligned}
\mathbf{I}_\Gamma &= \sigma_n^2\Gamma\Gamma^H,\\
\mathbf{R}_{c\Omega} &= \sum_{i=1}^{N_c} E\left(\left|a_{c,i}\right|^2\right)\left(\left[\mathbf{C}\Gamma_A\mathbf{v}\left(\varphi_{c,i}\right)\right] \otimes \left[\Gamma_P\mathbf{v}\left(f_{c,i}\right)\right]\right)\\
&\quad \times\left(\left[\mathbf{C}\Gamma_A\mathbf{v}\left(\varphi_{c,i}\right)\right] \otimes \left[\Gamma_P\mathbf{v}\left(f_{c,i}\right)\right]\right)^H\\
&= \left[\left(\mathbf{C}\Gamma_A\right) \otimes \Gamma_P\right] \times \sum_{i=1}^{N_c} E\left(\left|a_{c,i}\right|^2\right)\mathbf{v}\left(\varphi_{c,i}, f_{c,i}\right)\\
&\quad \mathbf{v}^H\left(\varphi_{c,i}, f_{c,i}\right)\left[\left(\mathbf{C}\Gamma_A\right) \otimes \Gamma_P\right]^H\\
&= \left(\mathbf{C} \otimes \mathbf{I}\right)\left(\Gamma_A \otimes \Gamma_P\right)\mathbf{R}_u\left(\Gamma_A \otimes \Gamma_P\right)^H\left(\mathbf{C} \otimes \mathbf{I}\right)^H\\
&= \mathbf{Z}\Gamma\mathbf{R}_c\left(\mathbf{Z}\Gamma\right)^H\\
&= \mathbf{\Omega}\mathbf{R}_c\mathbf{\Omega}^H,
\end{aligned} \tag{23}$$

with $\Gamma = \Gamma_A \otimes \Gamma_P$, $\Omega = \mathbf{Z}\Gamma$. In the light of the minimum variance distortionless response criterion, the optimal STAP weight vector can be estimated by

$$\mathbf{w}_{sm} = \frac{\mathbf{R}_{usm}^{-1}\mathbf{v}_{sm}}{\mathbf{v}_{sm}^H\mathbf{R}_{usm}^{-1}\mathbf{v}_{sm}}, \tag{24}$$

where $\mathbf{v}_{sm} = \mathbf{Z}\mathbf{v}_s(\varphi_t, f_t) = \Omega\mathbf{v}(\varphi_t, f_t)$ is the target space-time steering vector in the presence of mutual coupling. Typically, $\mathbf{R}_{usm}$ is estimated from the training samples by

$$\overline{R}_{usm} = \frac{1}{L}\sum_{i=1}^{L}\mathbf{x}_{u,i}\mathbf{x}_{u,i}^H, \tag{25}$$

where $\mathbf{x}_{u,i}, i = 1, \ldots, L$, presents training samples matrix with mutual coupling and L is the number of training samples.

Nevertheless, $\overline{R}_{usm}$ estimated by (25) is subject to the error within the limited snapshots. In order to analyze the estimation error of the training samples in (25), first, note that the vectorization form of estimation error $\mathbf{E} = \overline{R}_{usm} - \mathbf{R}_{usm}$ obeys an asymptotic zero-mean normal distribution, that is,

$$\mathrm{vec}\left(\mathbf{E}\right) \sim N\left(0, \mathbf{W}\right), \tag{26}$$

and therefore

$$\left\|\mathbf{W}^{-(1/2)}\mathrm{vec}\left(\mathbf{E}\right)\right\|_2^2 \sim \chi^2\left(N_S^2M_S^2\right), \tag{27}$$

where $\mathbf{W} = (1/L)\mathbf{R}_{usm}^T \otimes \mathbf{R}_{usm}$ and $\chi^2(N_S^2M_S^2)$ represents the asymptotic Chi-square distribution with N^2M^2 DOF.

It is remarkable that $\mathbf{R}_{usm}$ in the above derivation can be approximately estimated by (25), and the matrix $\mathbf{W}$ should be determined based on $\overline{R}_{usm}$ by

$$\overline{W} = \frac{1}{L}\overline{R}_{usm}^T \otimes \overline{R}_{usm}. \tag{28}$$

Hence, the matrix $\mathbf{W}$ in (26) and (27) is replaced by $\overline{W}$ in real calculations.

Note that

$$\left\|\overline{W}^{-(1/2)}\mathrm{vec}\left(\mathbf{E}\right)\right\|_2^2 \le \eta, \tag{29}$$

can be established with probability $1-p$ (approaching 1) on the basis of the properties of the squared distribution, where η can be counted by $N_S M_S$ and p. According to the theory of the low-rank matrix recovery, $\mathbf{R}_c$ can be estimated by solving the following minimization problem:

$$\begin{aligned} &\min \operatorname{rank}[\mathbf{R}_c] \\ &s.t. \left\| \overline{W}^{-(1/2)} \operatorname{vec}(\mathbf{E}) \right\|_2^2 \le \eta. \end{aligned} \tag{30}$$

However, the previous equation is a NP-hard problem. We can use trace norm instead of rank norm to avoid the nonconvex and obtain

$$\begin{aligned} &\min \operatorname{tr}[\mathbf{R}_c] \\ &s.t. \left\| \overline{W}^{-(1/2)} \operatorname{vec}(\mathbf{E}) \right\|_2^2 \le \eta. \end{aligned} \tag{31}$$

By introducing a Lagrangian multiplier, the previous equation can be reconstructed as

$$\min \operatorname{tr}[\mathbf{R}_c] + \frac{\lambda}{2} \left\| \overline{W}^{-(1/2)} \operatorname{vec}\left(\overline{R}_{usm} - \mathbf{R}_{c\Omega} - \mathbf{I}_\Gamma\right) \right\|_2^2, \tag{32}$$

which simplifies to

$$\begin{aligned} &\min \operatorname{tr}[\mathbf{R}_c] + \frac{\lambda}{2} \left\| \overline{W}^{-(1/2)} \operatorname{vec}\left(\overline{R}_{usm} - \mathbf{R}_{c\Omega} - \mathbf{I}_\Gamma\right) \right\|_2^2 \\ &= \min \operatorname{tr}[\mathbf{R}_c] + \frac{\lambda}{2} \Big[\operatorname{vec}^H \left(\overline{R}_{usm} - \mathbf{I}_\Gamma - \mathbf{R}_{c\Omega}\right) \\ &\quad \times \operatorname{vec}\Big(\left(\overline{R}_{usm} - \mathbf{I}_\Gamma\right)^{-1} \left(\overline{R}_{usm} - \mathbf{I}_\Gamma - \mathbf{R}_{c\Omega}\right) \left(\overline{R}_{usm} - \mathbf{I}_\Gamma\right)^{-1} \Big) \Big] \\ &= \min \operatorname{tr}[\mathbf{R}_c] + \frac{\lambda}{2} \Big[\operatorname{tr}\Big(\mathbf{R}_{c\Omega} \left(\overline{R}_{usm} - \mathbf{I}_\Gamma\right)^{-1} \mathbf{R}_{c\Omega} \left(\overline{R}_{usm} - \mathbf{I}_\Gamma\right)^{-1} \Big) \\ &\quad - 2\operatorname{tr}\Big(\mathbf{R}_{c\Omega} \left(\overline{R}_{usm} - \mathbf{I}_\Gamma\right)^{-1} \Big) \Big] \\ &= \min \operatorname{tr}[(\mathbf{I} - \lambda \mathbf{H}) \mathbf{R}_c] + \frac{\lambda}{2} \operatorname{tr}(\mathbf{R}_c \mathbf{H} \mathbf{R}_c \mathbf{H}), \end{aligned} \tag{33}$$

where $\mathbf{H} = \Omega^H \left(\overline{R}_{usm} - \mathbf{I}_\Gamma\right)^{-1} \Omega$.

It is worth noting that the CVX [22] can seek the solution of the above convex optimization problem. However, it needs high computational complexity when the system dimension is relatively large. Here, we try to find a fast and effective closed-form solution. According to the Karush–Kuhn–Tucker (KKT) conditions [23], (33) is equivalent to the following equation:

$$\mathbf{R}_c^* \left(\mathbf{H} \mathbf{R}_c \mathbf{H}\right) = \mathbf{R}_c^* \left(\lambda \mathbf{H} - \mathbf{I}\right), \tag{34}$$

where $\mathbf{R}_c^* (\mathbf{V}) = [v_{NM-1}, \ldots, v_{-(NM-1)}]^T$ and v_n can be obtained as

$$v_n = \begin{cases} \displaystyle\sum_{i=0}^{NM-1-n} V_{1+i,n+1+i}, & n = 0, \ldots, NM-1, \\ \displaystyle\sum_{i=0}^{NM-1-n} V_{1-n+i,1+i}, & n = -(NM-1), \ldots, -1. \end{cases} \tag{35}$$

Then, we can change the left-hand side of (34) to

$$\mathbf{R}_c^* \left(\mathbf{H} \mathbf{R}_c \mathbf{H}\right) = \underbrace{\begin{bmatrix} \mathbf{Z}^{(1)} \\ \mathbf{Z}^{(2)} \\ \vdots \\ \mathbf{Z}^{(M)} \end{bmatrix}}_{\mathbf{Z}} \begin{bmatrix} \mathbf{h}^{(M)} \\ \vdots \\ \mathbf{h}^{(2)} \\ \overline{h} \end{bmatrix}, \tag{36}$$

in which

$$\mathbf{Z}^{(n)} = \begin{bmatrix} \mathbf{R}_c^{*T} \left[\mathbf{G}_{:,\psi_1} \mathbf{G}_{\{NM+1-\psi_1\},:} \right] \\ \vdots \\ \mathbf{R}_c^{*T} \left[\mathbf{G}_{:,\psi_M} \mathbf{G}_{\{NM+1-\psi_M\},:} \right] \\ \mathbf{R}_c^{*T} \left[\mathbf{G}_{:,\zeta_1} \mathbf{G}_{\{NM+1-\zeta_1\},:} \right] \\ \vdots \\ \mathbf{R}_c^{*T} \left[\mathbf{G}_{:,\zeta_{M-1}} \mathbf{G}_{\{NM+1-\zeta_{M-1}\},:} \right] \end{bmatrix}, \qquad \mathbf{h} = \begin{bmatrix} \mathbf{h}^{(1)} \\ \mathbf{h}^{(2)} \\ \vdots \\ \mathbf{h}^{(N)} \end{bmatrix}, \tag{37}$$

with

$$\begin{aligned} \psi_q &= \bigcup_{m=1}^{M-n+1} \{(m-1)N + 1, \cdots, mN + 1 - q\}, \quad q = 1, \ldots, N, \\ \zeta_p &= \bigcup_{m=1}^{M-n} \{(m-1)N + 3 - p, \cdots, mN\}, \quad p = 1, \ldots, N-1, \\ \mathbf{h}^{(n)} &= \left[u_1^{(n)}, \ldots, u_N^{(n)}, v_1^{(n)}, \ldots, v_{N-1}^{(n)}\right]^T. \end{aligned} \tag{38}$$

According to (34) and (36), we obtain

$$\mathbf{R}_c^* (\mathbf{H}) = [\mathbf{Z}_1, \mathbf{Z}_2] \begin{bmatrix} \mathbf{h} \\ \overline{h} \end{bmatrix} = \mathbf{Z}_1 \mathbf{h} + \mathbf{Z}_2 \overline{h}, \tag{39}$$

where $\mathbf{Z}_1$ and $\mathbf{Z}_2$ obtained by evenly dividing $\mathbf{Z}$ have the same dimension and $\overline{h}$ stands for the conjugate of $\mathbf{h}$. Nevertheless, (39) can be represented in the following form:

$$\begin{bmatrix} \mathscr{R}\left(\mathbf{R}_c^* (\mathbf{H})\right) \\ \mathscr{I}\left(\mathbf{R}_c^* (\mathbf{H})\right) \end{bmatrix} = \begin{bmatrix} \mathscr{R}\left(\mathbf{Z}_1 + \mathbf{Z}_2\right) & \mathscr{I}\left(\mathbf{Z}_2 - \mathbf{Z}_1\right) \\ \mathscr{I}\left(\mathbf{Z}_1 + \mathbf{Z}_2\right) & \mathscr{R}\left(\mathbf{Z}_1 - \mathbf{Z}_2\right) \end{bmatrix} \begin{bmatrix} \mathscr{R}(\mathbf{h}) \\ \mathscr{I}(\mathbf{h}) \end{bmatrix}, \tag{40}$$

which results in

$$\begin{bmatrix} \mathscr{R}(\mathbf{h}) \\ \mathscr{I}(\mathbf{h}) \end{bmatrix} = \begin{bmatrix} \mathscr{R}\left(\mathbf{Z}_1 + \mathbf{Z}_2\right) & \mathscr{I}\left(\mathbf{Z}_2 - \mathbf{Z}_1\right) \\ \mathscr{I}\left(\mathbf{Z}_1 + \mathbf{Z}_2\right) & \mathscr{R}\left(\mathbf{Z}_1 - \mathbf{Z}_2\right) \end{bmatrix}^{\dagger} \begin{bmatrix} \mathscr{R}\left(\mathbf{R}_c^* (\mathbf{H})\right) \\ \mathscr{I}\left(\mathbf{R}_c^* (\mathbf{H})\right) \end{bmatrix}. \tag{41}$$

In this way, it is easy to calculate $\mathbf{h}$ from (41), which obtains the $\mathbf{R}_c(\overline{u}, t\overline{v})$ estimation. Finally, the optimal STAP filter weight vector can be described by $\mathbf{R}_c(\overline{u}, t\overline{v})$. It is worthy of note that we acquire the CCM of ULS if $\Gamma_A = \Gamma_P = \mathbf{I}$.

Moreover, when $\mathbf{C} = \mathbf{I}$, the mutual coupling is not considered in the proposed algorithm model.

4. Simulation Results and Discussion

In this section, we present numerical simulation results to verify the theoretical derivation made above and compare the TCMR-STAP with the existing methods including the RCML-STAP [24], mDT-STAP [5], JDL-STAP [6], and SMI-STAP [2]. The parameters of the radar system are assumed as $\lambda = 0.05m$, $d = \lambda/2$, $T_r = 0.25$ms, $v = 50m/s$, $\sigma_n^2 = 1$, $N_c = 361$, and clutter to noise ratio CNR = 30dB. In these examples, one target whose normalized angle and Doppler, respectively, are set to 0.1 and −0.2 is present. All simulation results are average over 100 Monte Carlo experiments.

4.1. Performance of TCMR-STAP with ULS. We begin by analyzing the presented approach feasibility and efficiency in small samples, set $M = N = 10$ in the ULS. As a comparison, the output SINR versus the number of training samples and the normalized Doppler frequency are shown for performance evaluation. Figure 1 reveals the output SINR of five methods by varying samples size from 2 to 200 in the target normalized Doppler frequency −0.2. As intuitively expected, the steady SINR performance increases with sample number except for the SMI-STAP [2]. SMI have a dip due to numerical instabilities in the $L = 100$ training regime. It is seen that the mDT-STAP, JDL-STAP, and SMI-STAP are able to achieve poor performance when very small snapshots are collected, and the RCML-STAP enjoys higher precision among the above three methods. However, the performance of TCMR-STAP is the least affected by the number of training samples among the compared methods, which can exhibit remarkably good performance even when there are only several training samples and also converge much fastest than other schemes. In particular, the TCMR-STAP is able to work in limited samples scenario and solves the radar performance degradation caused by the lack of samples.

Moreover, we compare the SINR performance against the normalized Doppler frequency of the TCMR-STAP with others in $L = 100$, as shown in Figure 2. The plot shows that the TCMR-STAP outperforms other algorithms in the Doppler bins, and forms a deep null to cancel the main clutter field.

4.2. Performance of TCMR-STAP with SLS. Here, we compare the SINR and space-time beampatterns in order to reflect the advantages of our method in SLS with $\mathbf{A} = \mathbb{P} = \{0, 1, 4, 7, 9\}$ and $L = 100$. First, we evaluate the SINR performance against the normalized Doppler frequency for the proposed TCMR-STAP with SLS (SLS-TCMR-STAP) under $N = M = 5$, which is shown in Figure 3. The plot shows that our method outperforms other algorithms in the Doppler domain and has a deep null in the main clutter field. The SLS-TCMR-STAP, on the other hand, has approximately the same performance as the TCMR-STAP with ULS (ULS-TCMR-STAP) with $N = M = 10$.

To further illustrate the superiorities of TCMR-STAP, we compare the space-time beampatterns of the SMI-STAP and TCMR-STAP and get satisfactory results. Specifically,

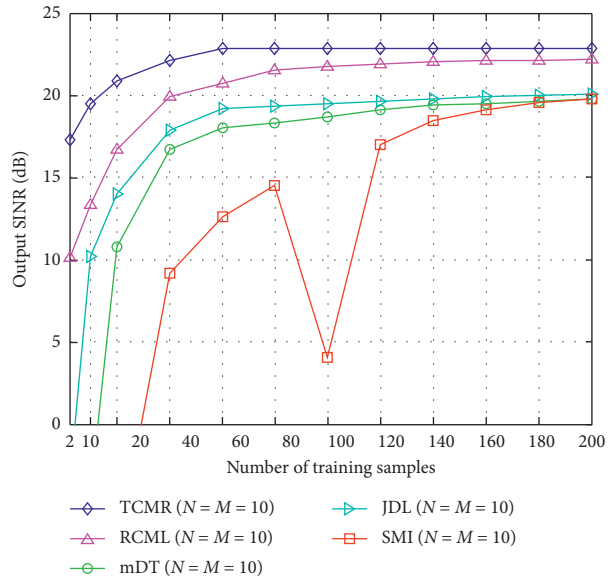

Figure 1: SINR versus the number of training samples.

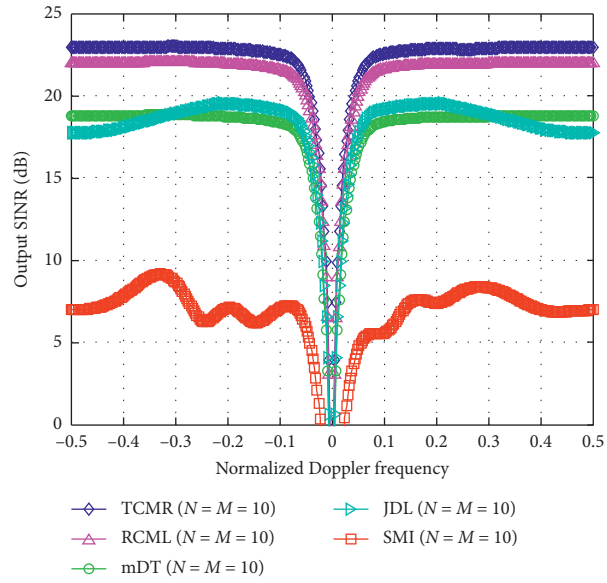

Figure 2: SINR versus the normalized Doppler frequency ($L = 100$).

Figures 4(a)–4(c) are corresponding to the SMI-STAP with ULS ($N = M = 5$), SMI-STAP with ULS ($N = M = 10$), and SLS-TCMR-STAP ($N = M = 5$), respectively. It is seen that all of the three methods can fully suppress the clutter and make a maximum peak at the target position. Nevertheless, the angle and Doppler resolutions of the SLS-TCMR-STAP are better than those of the SMI-STAP with ULS under the same N and M owing to the increased DOF. Moreover, the SLS-TCMR-STAP is notably better than the SMI-STAP with ULS ($N = M = 10$), as shown in Figure 5.

We then give the beampatterns in spatial and Doppler domains. Figure 6(a) shows the beampatterns in the spatial domain at the target normalized Doppler frequency while Figure 6(b) plots the beampatterns in the Doppler domain at

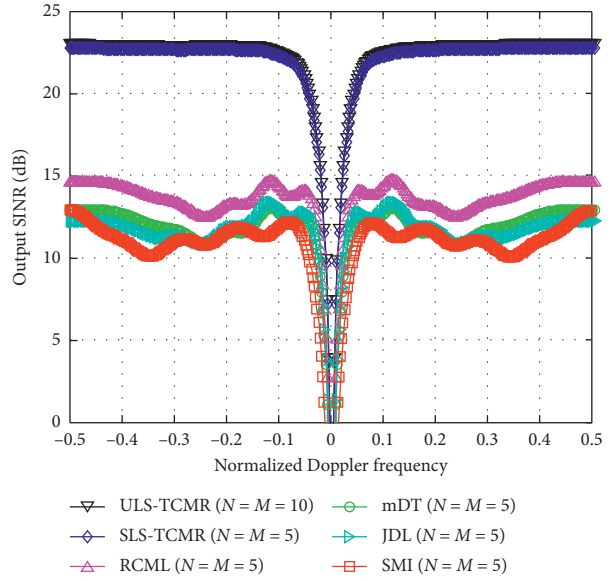

Figure 3: SINR versus the normalized Doppler frequency ($L = 100$).

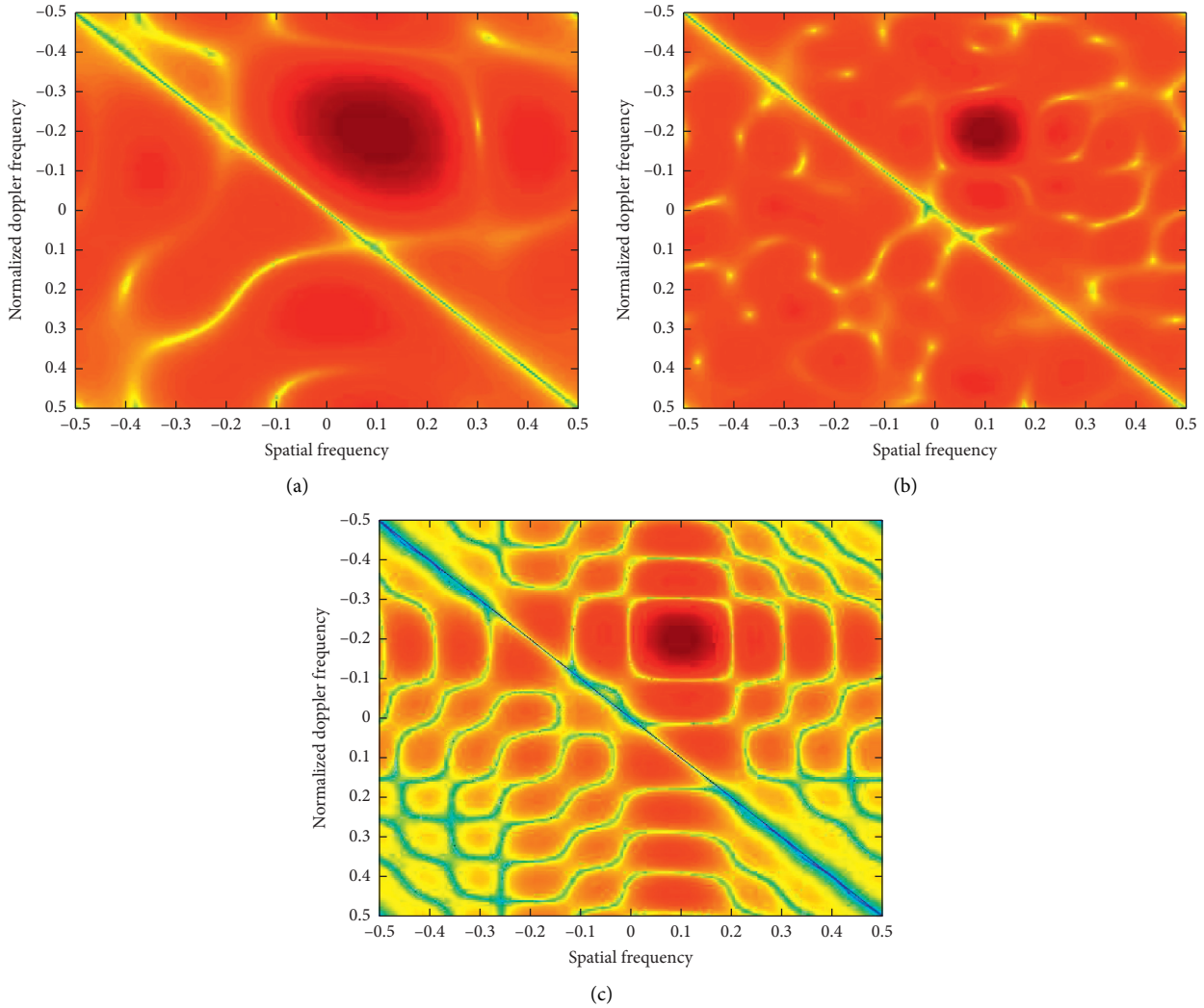

Figure 4: Beampatterns ($L = 100$). (a) The SMI-STAP with ULS and $N = M = 5$. (b) The SMI-STAP with ULS and $N = M = 10$. (c) The SLS-TCMR-STAP with $N = M = 5$.

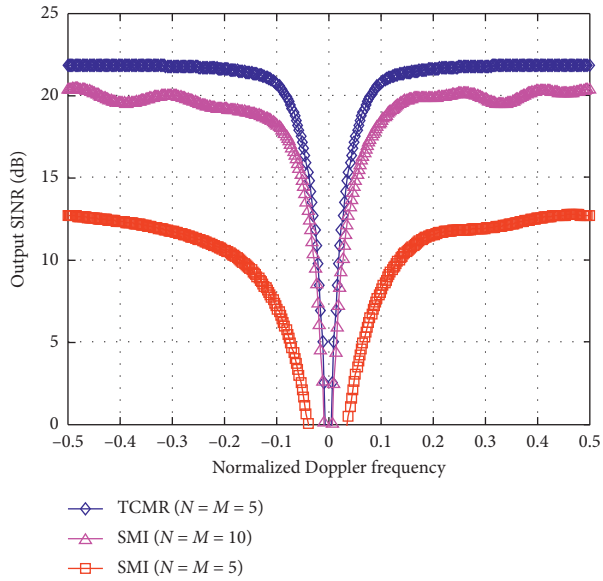

Figure 5: SINR versus the normalized Doppler frequency ($L = 100$).

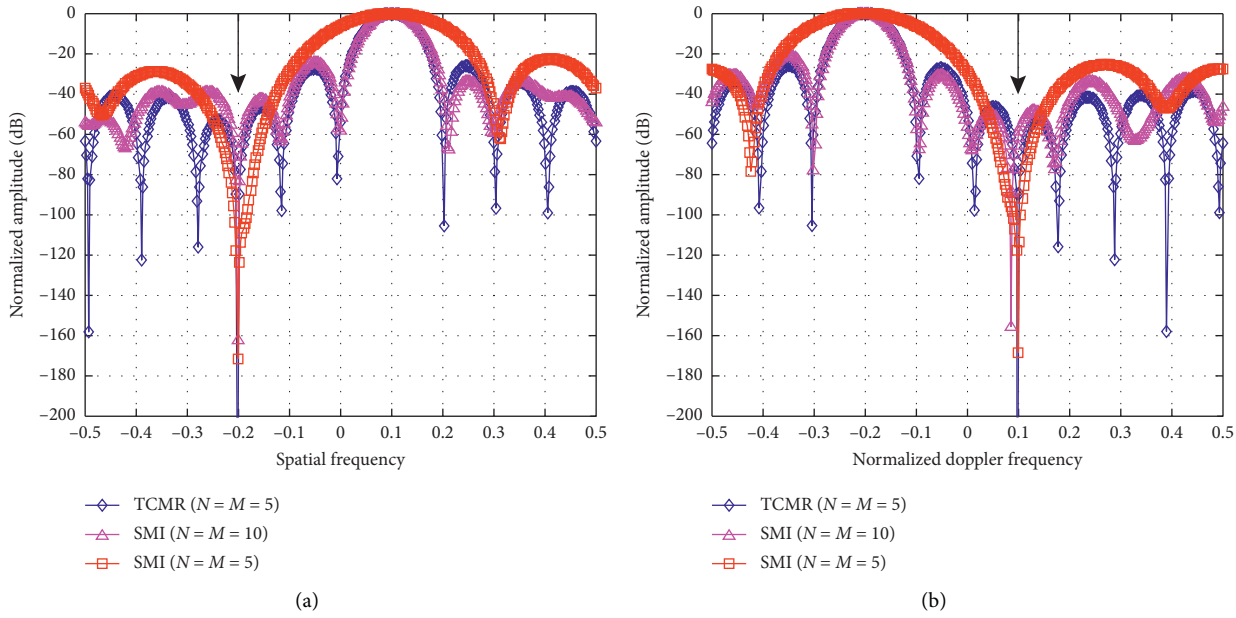

Figure 6: Beampatterns ($L = 100$). (a) Spatial domain. (b) Doppler domain.

the target spatial frequency. It is observed that the SLS-TCMR-STAP ($N = M = 5$) can obtain the same angle-Doppler resolution as the SMI-STAP with ULS ($N = M = 10$), but its sidelobe level is relatively better. It means that the SLS system can provide larger DOF in the virtual domain and improve the space-time resolution with fewer hardware resources and power consumption. On the other hand, it is shown the TCMR-STAP has a stronger capability of clutter suppression by means of analyzing the plots.

4.3. Performance of TCMR-STAP with Mutual Coupling. In the experiment, we evaluate the mutual coupling of the SLS-TCMR-STAP with $M = N = 5$. Then, we also show the mutual coupling effect on the beampatterns in Figure 7, where the mutual coupling model is based on (18) with $c_1 = 0.5e^{(j\pi/4)}$, $c_2 = 0.25e^{j0.7\pi}$, $c_3 = 0.5e^{j0.7\pi}/3$, and $B = 3$. The number of samples is $L = 200$. The SMI-STAP with ULS possess no deep notch in the main clutter region, implying it suffers from the severe mutual coupling effect, as shown in Figure 7(a). For the SLS-TCMR-STAP, since the inter-sensors spacing is increased, the mutual coupling can be further reduced; as a result, its weight functions can be lower than those of the ULS shown in Figure 7(b). Therefore, the SLS is emphasized on the importance of the comprehensive balance between the DOF and the mutual coupling. Figure 8 shows the beampatterns in spatial and Doppler domain in the presence of mutual coupling. As shown in Figure 8, the

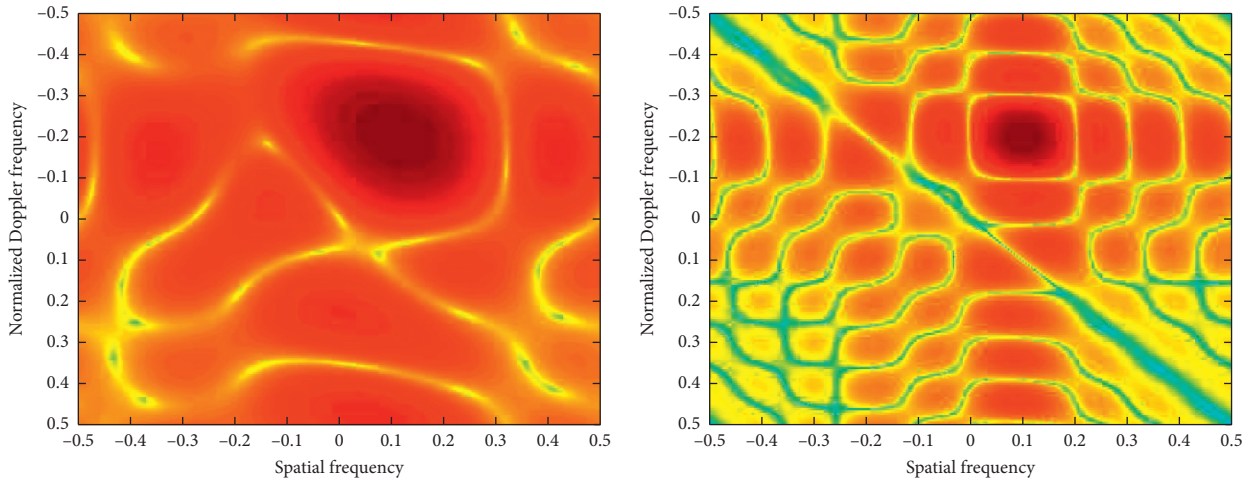

Figure 7: Beampatterns ($L = 200$). (a) The SMI-STAP with ULS and $N = M = 5$. (b) The SLS-TCMR-STAP with $N = M = 5$.

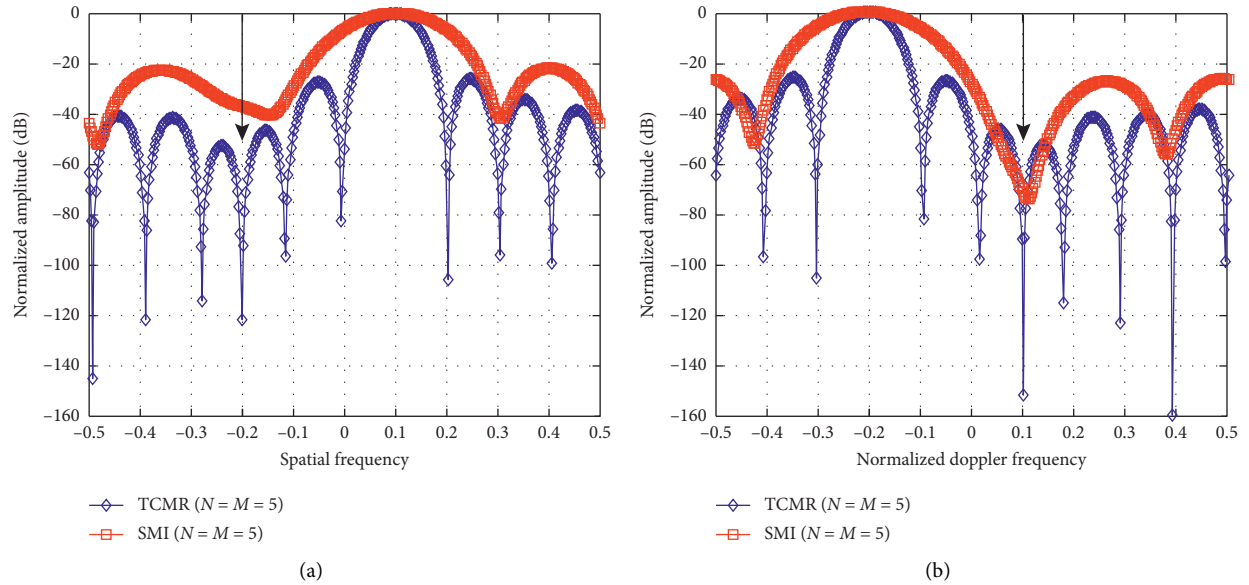

Figure 8: Beampatterns ($L = 200$). (a) Spatial domain. (b) Doppler domain.

SMI-STAP with ULS does not have a deep notch in the main clutter region; it means that it cannot appropriately work in the presence of mutual coupling.

5. Conclusion

The traditional training samples mean the method is effective in estimating the CNCM, but it is difficult to obtain the CNCM accurately with limited training samples. This paper has proposed a robust STAP algorithm for airborne radar against unknown mutual coupling considering the Toeplitz covariance matrix reconstruction, which can be applied to the ULS and SLS system to solve the problem of insufficient training samples and reduce the mutual coupling effect. In particular, we first adopt the structure for CCM recovery based on the prior knowledge of noise and then relax it by using the trace norm instead of the rank norm. The closed-form solution of the problem is derived, and a feasible implementation algorithm's fast solution is provided. Moreover, under the conditions fixed in the number of sensors and pulses, the system can obtain higher DOF by applying the difference operation in the SLS and reduce the mutual coupling effect. The simulation and experiment results show that the proposed method has high estimation precision, even in small samples. Compared with the existing algorithms, the TCMR-STAP possesses much better performance of clutter suppression, especially a very small number of training samples. Compared with the existing

algorithms for the ULS in the fixed number of sensors and pulses, the TCMR-STAP shows a greater DOF and decreases the mutual coupling. In future research, we will consider the target-like interference and assess the performance of the TCMR-STAP with the measured data.

Data Availability

The datasets supporting the conclusions of this article are generated using MATLAB software by authors according to the radar parameters described in the manuscript.

Conflicts of Interest

The authors declare no conflicts of interest.

Acknowledgments

This work was supported by the National Natural Science Foundation of China (Grant no. 61806046).

References

[1] K. Lee and J. Lee, "Design and evaluation of symmetric space-time adaptive processing of an array antenna for precise global navigation satellite system receivers," *IET Signal Processing*, vol. 11, no. 6, pp. 758–764, 2017.

[2] R. Klemm, *Principles of Space-Time Adaptive Processing*, IET, London, UK, 3rd edition, 2006.

[3] Y. Feng, T. Shan, S. H. Liu, and R. Tao, "Interference suppression using joint spatio-temporal domain filtering in passive radar," in *Proceedings of the IEEE Radar Conference (RadarCon)*, pp. 1156–1160, Arlington, VA, USA, May 2015.

[4] M. Liu, L. Zou, X. Yu, Y. Zhou, X. Wang, and B. Tang, "Knowledge aided covariance matrix estimation via Gaussian kernel function for airborne SR-STAP," *IEEE Access*, vol. 8, pp. 5970–5978, 2020.

[5] Z. C. Yang, Y. L. Qin, R. C. D. Lamare, H. Q. Wang, and X. Li, "Sparsity-based direct data domain space-time adaptive processing with intrinsic clutter motion," *Circuits Syst. Signal Process.*vol. 36, no. 1, pp. 1–28, 2017.

[6] W. Feng, Y. Zhang, and X. He, "Clutter rank estimation for reduce-dimension space-time adaptive processing MIMO radar," *IEEE Sensors Journal*, vol. 17, no. 2, pp. 238-239, 2017.

[7] W. Zhang, M. Han, Z. He, and H. Li, "Data-dependent reduced-dimension STAP," *IET Radar, Sonar & Navigation*, vol. 13, no. 8, pp. 1287–1294, 2019.

[8] X. R. Wang, E. Aboutanios, and M. G. Amin, "Reduced-rank STAP for slow-moving target detection by antenna-pulse selection," *IEEE Signal Processing Letters*, vol. 22, no. 8, pp. 1156–1160, 2015.

[9] D. Cristallini and W. Burger, "A robust direct data domain approach for STAP," *IEEE Transactions on Signal Processing*, vol. 60, no. 3, pp. 1283–1294, 2012.

[10] Z. Wang, Y. Wang, K. Duan, and W. Xie, "Subspace-augmented clutter suppression technique for STAP radar," *IEEE Geoscience and Remote Sensing Letters*, vol. 13, no. 3, pp. 462–466, 2016.

[11] M. Riedl and L. C. Potter, "Knowledge-aided Bayesian space-time adaptive processing," *IEEE Transactions on Aerospace and Electronic Systems*, vol. 54, no. 4, pp. 1850–1861, 2018.

[12] Y. Gao, H. Li, and B. Himed, "Knowledge-aided range-spread target detection for distributed MIMO radar in nonhomogeneous environments," *IEEE Transactions on Signal Processing*, vol. 65, no. 3, pp. 617–627, 2017.

[13] G. Foglia, C. Hao, A. Farina, G. Giunta, D. Orlando, and C. Hou, "Adaptive detection of point-like targets in partially homogeneous clutter with symmetric spectrum," *IEEE Transactions on Aerospace and Electronic Systems*, vol. 53, no. 4, pp. 2110–2119, 2017.

[14] S. Bidon, O. Besson, and J.-Y. Tourneret, "Knowledge-aided STAP in heterogeneous clutter using a hierarchical Bayesian algorithm," *IEEE Transactions on Aerospace and Electronic Systems*, vol. 47, no. 3, pp. 1863–1879, 2011.

[15] C. Hao, D. Orlando, G. Foglia, and G. Giunta, "Knowledge-based adaptive detection: joint exploitation of clutter and system symmetry properties," *IEEE Signal Processing Letters*, vol. 23, no. 10, pp. 1489–1493, 2016.

[16] T. Jian, G. Liao, Y. He, J. Guan, and Y. Dong, "Adaptive persymmetric detector of generalised likelihood ratio test in homogeneous environment," *IET Signal Processing*, vol. 10, no. 2, pp. 91–99, 2016.

[17] A. Haimovich, "Low-complexity algorithms for low rank cutter parameters estimation in radar systems," *IEEE Transactions on Signal Processing*, vol. 64, no. 8, pp. 1986–1998, 2016.

[18] Y. Wang and Z. He, "Thinned knowledge-aided STAP by exploiting structural covariance matrix," *IET Radar, Sonar & Navigation*, vol. 11, no. 8, pp. 1266–1275, 2017.

[19] C.-L. Liu and P. P. Vaidyanathan, "Super nested arrays: linear sparse arrays with reduced mutual coupling-Part I: fundamentals," *IEEE Transactions on Signal Processing*, vol. 64, no. 15, pp. 3997–4012, 2016.

[20] M. Liu, X. Wang, and L. Zou, "Robust STAP with reduced mutual coupling and enhanced DOF based on super nested sampling structure," *IEEE Access*, vol. 7, pp. 175420–175428, 2019.

[21] Y. H. Lin, M. Li, R. L. Haupt, and Y. J. Guo, "Synthesizing shaped power patterns for linear and planar antenna arrays including mutual coupling by refined joint rotation/phase optimization," *IEEE Transactions on Antennas and Propagation*, vol. 68, no. 6, pp. 4648–4657, 2020.

[22] M. Grant, S. Boyd, and Y. Ye, *CVX: Matlab Software for Disciplined Convex Programming*, CVX Research, Inc., Austin, TX, USA, 2008.

[23] X. Yu, G. Cui, J. Yang, J. Li, and L. Kong, "Quadratic optimization for unimodular sequence design via an ADPM framework," *IEEE Transactions on Signal Processing*, vol. 68, pp. 3619–3634, 2020.

[24] B. Kang, V. Monga, and M. Rangaswamy, "Rank-constrained maximum likelihood estimation of structured covariance matrices," *IEEE Transactions on Aerospace and Electronic Systems*, vol. 50, no. 1, pp. 501–515, 2014.